Stanford Exploration Project, Report 103, April 27, 2000, pages 205–324

Stanford Exploration Project, Report 103, April 27, 2000, pages 205–324

Data alignment with non-stationary shaping filters

James Rickett[1]

ABSTRACT

Cross-correlation provides a method of calculating a static shift between two datasets. By cross-correlating patches of data, I can calculate a "warp function" that dynamically aligns the two datasets. By exploiting the link between cross-correlation and shaping filters, I calculate warp functions in a more general way, leveraging the full machinery of geophysical estimation. I compare warp functions, derived by the two methods, for simple one and two-dimensional applications. For the one-dimensional well-tie example, shaping filters gave significantly improved results; however, for the two dimensional residual migration example, the cross-correlation technique gave the better results. I also explain how the helical transform allows the problem of finding a shaping filter to be formulated as an auto-regression.

INTRODUCTION

In both the fields of medical and seismic imaging, automated interpretation of volumetric data is becoming very important. A classical medical imaging problem is how to deform a template image to match an observed image (Kjems et al., 1996). This deformation process is also known as *warping* (Wolberg, 1990), and is the subject of a large literature within the medical imaging community that is reviewed by Toga and Thompson (1998).

Applications of warping, however, are not limited to medical imaging: automated coregistration algorithms may be useful whenever multiple datasets need to be compared directly with one another. In the field of seismic exploration, Grubb and Tura (1997) used a warping algorithm when estimating AVO uncertainties: they migrated a field with multiple equiprobable velocity fields, and colocated the images with cross-correlation derived warp functions. In another seismic application, Rickett and Lumley (1998) included warping as part of a time-lapse reservoir monitoring cross-equalization flow, specifically to address the effects of migrations with different velocity fields. They also found a link between statistically derived warp functions and deterministic residual migration (Rothman et al., 1985) or velocity continuation (Fomel, 1997a) operators.

[1]**email:** james@sep.stanford.edu

Warping: a two step process

Warping is nothing more than resampling of an image in a stretched coordinate system. I split the warping operation into two stages: firstly, the determination of the new coordinate system, and secondly, the spatial and/or temporal resampling.

The second step, the resampling, is just an interpolation operation. It is no more complex than applying normal moveout (NMO), for example. However, as with other resampling operators, the choice of interpolation (nearest-neighbour, linear, band-limited etc.) may affect the quality of results.

The more challenging problem is how do we determine the new coordinate system? Or equivalently, how do we determine the warp function itself?

Calculation of the warp function

The previous authors (Grubb and Tura, 1997; Rickett and Lumley, 1998) determined the warp function by calculating local cross-correlation functions at certain node points within the image space. The warp function at those node points is then taken to be the lag associated with the maxima of the cross-correlelograms. Node values may then be smoothed and interpolated to fill the image volume.

Unfortunately because seismic data is band-limited, cross-correlelograms have multiple local maxima, and in noisy data situations, the maxima may have similar amplitude. Simply picking maxima is, therefore, prone to cycle-skipping problems. The problem of cycle-skipping is fundamental to the process of automated (and even manual) seismic interpretation. Rickett and Lumley (1998) addressed it by heavy smoothing and median filtering of the warp functions before the image resampling itself.

In this paper, I exploit the link between shaping filters and cross-correlation functions to incorporate the smoothing within the matching process. I pick shaping filter maxima as opposed to cross-correlelogram maxima, reducing the need for ad hoc smoothing after the fact.

THEORY

Cross-correlation and shaping filters

A simple numerical way to find a static shift between two traces is to find the maximum of their cross-correlation function. The relative shift is the corresponding cross-correlation lag. Shaping filters are closely related to the simple cross-correlation function, and can also be used to measure relative shifts.

The shaping filter designed to match a first dataset, $\mathbf{d}_1$, with a second dataset, $\mathbf{d}_2$, can be defined as the filter, **a** that minimizes the norm of the objective function,

$$O(\mathbf{a}) = ||\, \mathbf{a} * \mathbf{d}_1 - \mathbf{d}_2 \,||, \qquad (1)$$

where $*$ denotes convolution. Equation (1) is very general: it implies nothing about either the choice of norm, or the dimensionality of $\mathbf{d}_1$, $\mathbf{d}_2$ or the filter **a**.

The classical discrete solution (Robinson and Treitel, 1980) to equation (1), which minimizes $O(\mathbf{a})$ in the L_2 sense, can be written as

$$\mathbf{a} = \left(\mathbf{D}_1^{\mathrm{T}} \mathbf{D}_1\right)^{-1} \mathbf{D}_1^{\mathrm{T}} \mathbf{d}_2. \qquad (2)$$

In this paper, I will use the convention that a bold upper case letter represents the operator that describes convolution with the filter represented by the corresponding lower case letter. For example, $\mathbf{D}_1$ represents the matrix which describes convolution with the dataset, $\mathbf{d}_1$, and $\mathbf{D}_2$ describes the matrix which represents convolution with $\mathbf{d}_2$. Multi-dimensionality in equation (2) is built into the definition of the convolution matrices.

Equation (2) implies that the optimal shaping filter, **a**, is given by the cross-correlation of $\mathbf{d}_1$ with $\mathbf{d}_2$, filtered by the inverse of the auto-correlation of $\mathbf{d}_1$. Equation (2) provides an alternative method of computing a cross-correlation function: firstly calculate an L_2 shaping filter to link one dataset with the other; secondly, recolor the filter with the auto-correlation of the first dataset.

It is not immediately clear why we would ever want to do this in practice, since the first step of computing a shaping filter is to compute a cross-correlation. However, shaping filter estimation can leverage the well-developed machinery of geophysical inversion (Claerbout, 1999) in a number of ways; for example, we may include non-stationarity, a different choice of norm, or different types of regularization in an alternative definition of a shaping filter.

The new algorithm for finding a warp function has three steps. First, estimate a non-stationary shaping filter. Second, recolor the shaping filter by convolving it with the autocorrelation of $\mathbf{d}_1$. Finally pick the maxima of the recolored shaping filters.

Adaptive shaping filters

The first step is to consider non-stationary shaping filters. Experience with missing data problems (Crawley et al., 1998; Crawley, 1999b) has shown that working with smoothly-varying non-stationary filters often gives better results than working with filters that are stationary within small patches.

With a non-stationary convolution filter, **f**, the shaping filter regression equations,

$$\mathbf{A}_1 \mathbf{f} - \mathbf{a}_2 = \mathbf{0}, \qquad (3)$$

are massively underdetermined since there is a potentially unique impulse response associated with every point in the dataspace (Rickett, 1999). We need constraints to ensure the filters vary-smoothly in some manner. The simplest regularization scheme involves applying a generic data-space roughening operator, **R**, to the non-stationary filter coefficients. **R** can be a simple derivative operator, for example. This leads to the set of equations,

$$\mathbf{A}_1 \mathbf{f} - \mathbf{a}_2 = \mathbf{0} \tag{4}$$

$$\epsilon \, \mathbf{R}\mathbf{f} = \mathbf{0} \,. \tag{5}$$

By making the change of variables, $\mathbf{q} = \mathbf{R}\,\mathbf{f}$ (Fomel, 1997b), we get the following system of equations,

$$\mathbf{A}_1 \mathbf{R}^{-1} \mathbf{q} - \mathbf{a}_2 = \mathbf{0} \tag{6}$$

$$\epsilon \, \mathbf{q} = \mathbf{0} \,. \tag{7}$$

Equations (6) and (7) describe a preconditioned linear system of equations, the solution to which converges rapidly under an iterative conjugate-gradients solver. In practice, I set $\epsilon = 0$, and keep the filters smooth by restricting the number of iterations (Crawley, 1999a).

Shaping filers on a helix

In a helical coordinate system (Claerbout, 1997), calculation of shaping filters can be formulated as an autoregression. If we concatenate the two datasets being matched, and ensure that filter lags span the two datasets, then the shaping filter is identical to the prediction-filter that is used to predict the second dataset from the first. This convenient observation allows reuse of both codes and concepts.

APPLICATIONS

I demonstrate the difference in results obtained by cross-correlations and non-stationary shaping filters on two simple examples: firstly, a 1-D well-tie problem, and secondly a 2-D statistical residual migration. Both methods extend naturally to higher dimensions as well; however, while the cost of the cross-correlation method is proportional to the number of filter coefficients, N_f, the cost of the shaping filter method is proportional to N_f^2, since the number of iterations depends on the number of filter coefficients.

One-dimensional well-ties

Figure 1 shows a seismic section from which I drew two hypothetical sonic logs. The task was then to match them to each other. The fault that cuts through the section and the poor data quality in the lower part cause problems from matching algorithms.

Figures 2 and 3 compare the results of the two warping algorithms. The shaping filters themselves change more smoothly as a function of time than the local cross-correlelograms. The warped difference (trace 3 in both figures) also contains less energy in Figure 3 than Figure 2 indicating the shaping filters have found a better match. Clip levels for the wiggle displays are the same for both Figures 2 and 3.

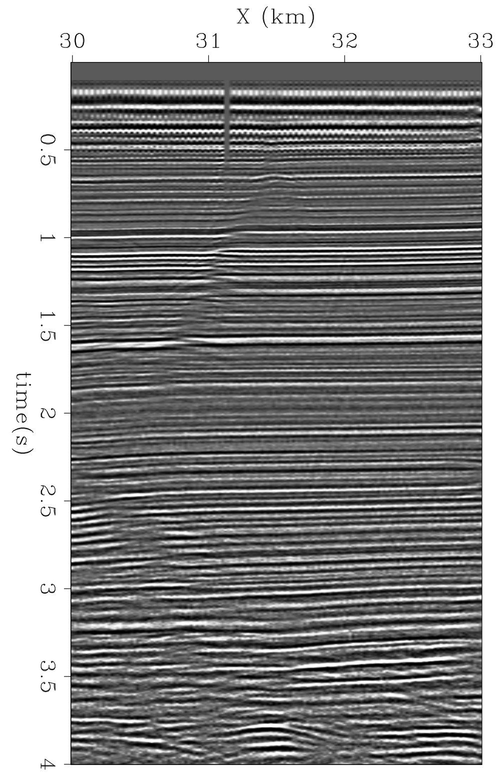

Figure 1: Seismic section from which two hypothetical sonic logs were drawn. $\mathbf{d}_1$ was drawn at X=31 km and $\mathbf{d}_2$ was drawn at X=32 km. james2-data [ER]

Two-dimensional residual migration

The two panels in Figure 4 show the same 2-D section from a 3-D depth migration of the Elf L7D dataset (Vaillant, 1999), after residual migration with two different residual velocity ratios (Sava, 2000) and conversion to traveltime depth. I converted to traveltime depth to avoid remove systematic gross kinematic changes in depth, while leaving changes in kinematics due to imaging differences.

Figure 5 compares the raw difference between the two panels in Figure 4 with the difference after warping with the cross-correlation algorithm, and the shaping filter algorithm. Comparing panel (a) and panel (b) shows the energy in the cross-correlation difference section has decreased significantly, and the algorithm has aligned the main events well. The RMS amplitude decreased a factor of 0.6. On the other hand, comparing panels (a) and (c) shows the shaping filters have not nearly been as successful: although the flanks of the salt have been well aligned, other parts of the section are less well aligned than before warping. The RMS amplitude in panel (c) has only been reduced by a factor of 0.8.

Although I tried a range of parameters, the shaping filter results could probably be improved by tweaking them further. There are many possible options with regard choice of roughening filter and number of iterations, and it is difficult to find the best set.

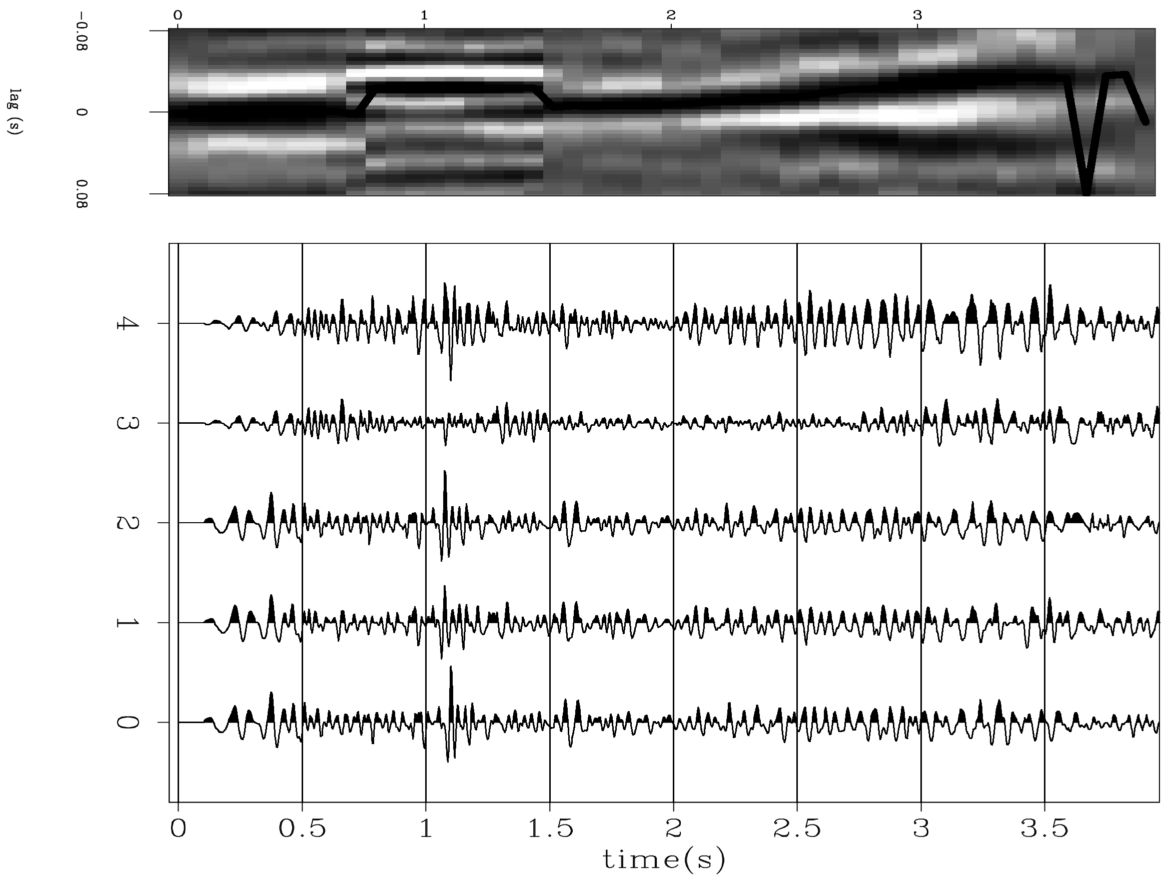

Figure 2: Cross-correlation results. The top panel shows cross-correlelograms and picked maxima. The bottom panel shows $\mathbf{d}_1$ (0), $\mathbf{d}_2$ (1), warped $\mathbf{d}_1$ (2), $\mathbf{d}_2 -$ warped $\mathbf{d}_1$ (3), and $\mathbf{d}_2 - \mathbf{d}_1$ (4). james2-xcorr1 [ER]

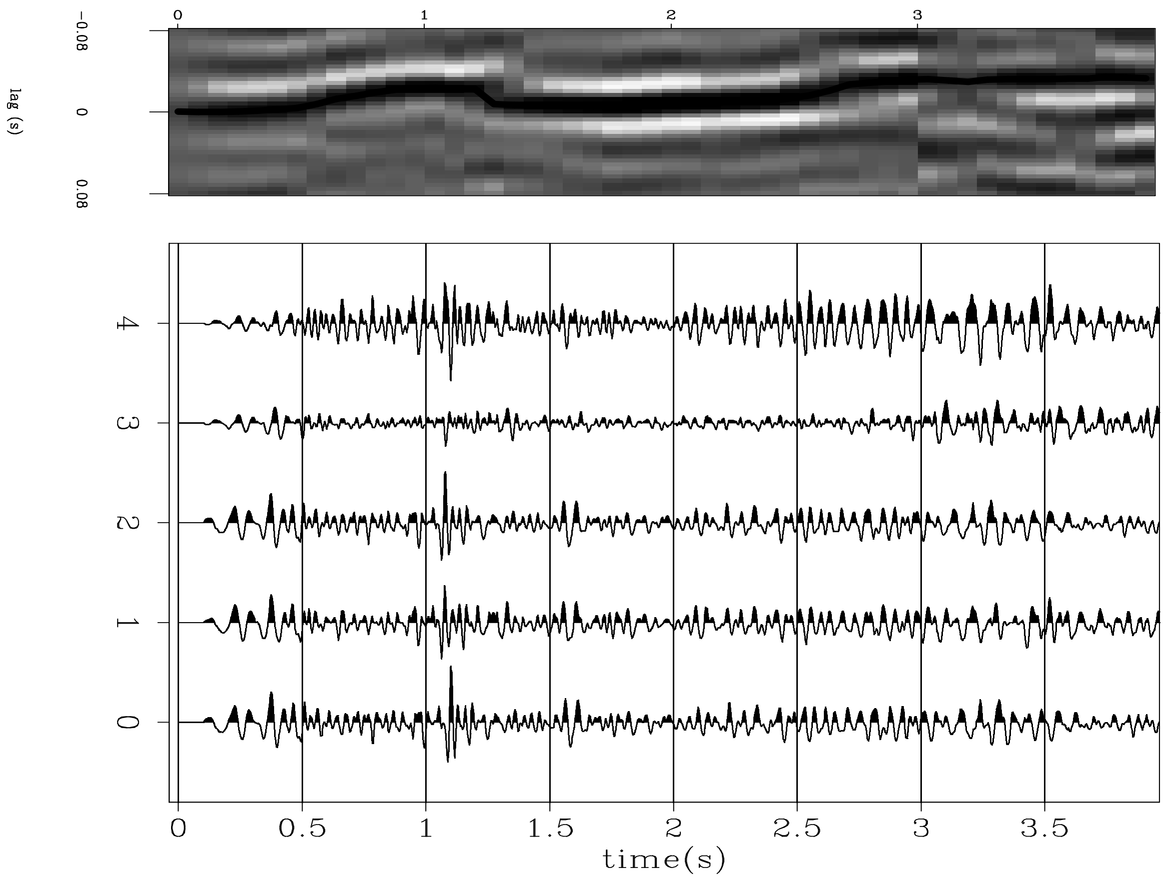

Figure 3: Non-stationary shaping filter results. The top panel shows cross-correlelograms and picked maxima. The bottom panel shows $\mathbf{d}_1$ (0), $\mathbf{d}_2$ (1), warped $\mathbf{d}_1$ (2), $\mathbf{d}_2 -$ warped $\mathbf{d}_1$ (3), and $\mathbf{d}_2 - \mathbf{d}_1$ (4). james2-xcorr2 [ER]

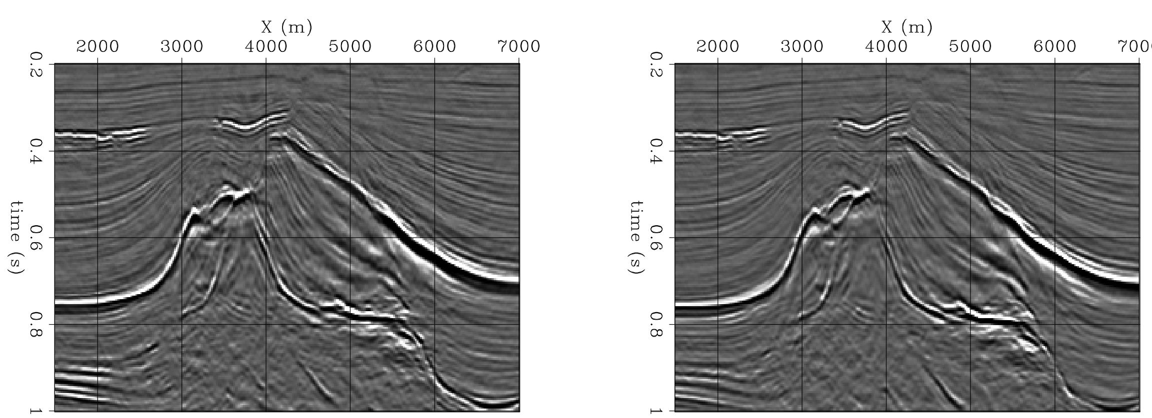

Figure 4: Seismic sections extracted from the Elf L7D dataset after residual migration with $v_{\text{ratio}} = 0.96$ and $v_{\text{ratio}} = 1.02$ and conversion from depth to traveltime depth. james2-elfpanels [ER]

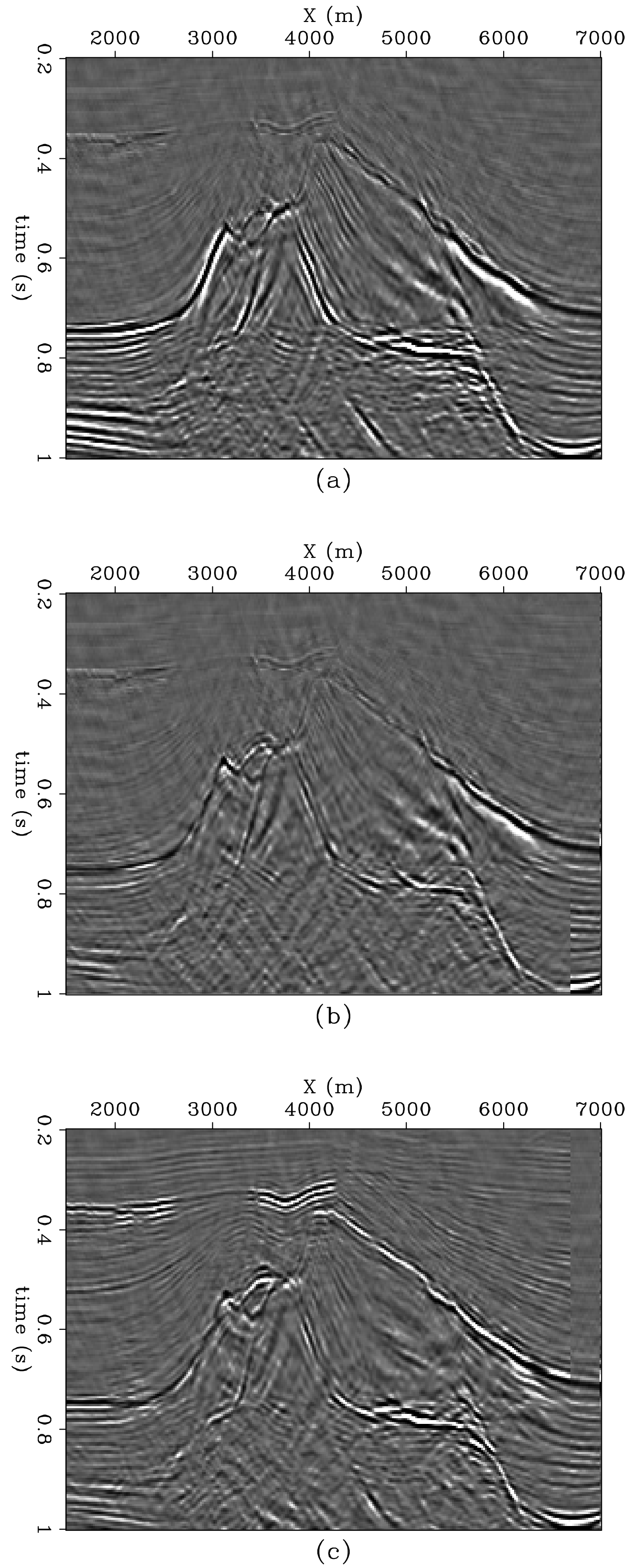

Figure 5: (a) Raw difference between the two panels in Figure 4. (b) The difference after warping with the cross-correlation algorithm. (c) The difference after warping with the shaping filter algorithm. james2-diff [CR]

FURTHER WORK

Derivation of a warp function is fundamentally a non-linear process, and I am never going to be able to escape that fact. However, there are tractable and non-tractable non-linear problems that we have some experience with. By formulating the problem of finding a warp function in the framework of geophysical estimation theory, I have opened up many possible avenues of exploration.

A big problem is the presence of secondary maxima that confuse the picking operation; ideally we would like to pick from functions with unique maxima. We may be able to achieve this goal by imposing a minimum-entropy condition (Thorson, 1984) on the shaping filter regularization (model-space residual). In practice, however, this may have convergence problems, and we may be better off with an L_1 norm on the model-space residual (Nichols, 1994), or even the Huber norm (Guitton, 2000).

CONCLUSIONS

Shaping filters are closely related to cross-correlelograms, and therefore can be used to calculate kinematic misalignments between two similar datasets. I demonstrate the use of shaping filters to calculate a dynamic "warp" function that maps one dataset to another. Shaping filters can leverage the power of geophysical estimation theory, which potentially may help avoid problems associated with noisy data to provide improved estimates of multi-dimensional warp functions.

I compared results of warping with a function derived from shaping filters with results from a warp function derived from cross-correlelograms. For the one-dimensional well-tie example, the shaping filters gave encouraging results; however, for the two-dimensional example the cross-correlation technique gave better results.

ACKNOWLEDGEMENTS

Thanks to Paul Sava for providing the residual migrations for the 2-D example.

REFERENCES

Claerbout, J., 1997, Preconditioning and scaling: SEP–**94**, 137–140.

Claerbout, J., 1999, Geophysical estimation by example: Environmental soundings image enhancement: Stanford Exploration Project, http://sepwww.stanford.edu/sep/prof/.

Crawley, S., Clapp, R., and Claerbout, J., 1998, Decon and interpolation with nonstationary filters: SEP–**97**, 183–192.

Crawley, S., 1999a, Interpolating missing data: convergence and accuracy, t and f: SEP–**102**, 77–90.

Crawley, S., 1999b, Interpolation with smoothly nonstationary prediction-error filters: SEP–**100**, 181–196.

Fomel, S., 1997a, Velocity continuation and the anatomy of prestack residual migration: 67th Annual Internat. Mtg., Soc. Expl. Geophys., Expanded Abstracts, 1762–1765.

Fomel, S., 1997b, On model-space and data-space regularization: A tutorial: SEP–**94**, 141–164.

Grubb, H., and Tura, A., 1997, Interpreting uncertainty measures for AVO migration/inversion: 67th Annual Internat. Mtg., Soc. Expl. Geophys., Expanded Abstracts, 210–213.

Guitton, A., 2000, Implementation of a nonlinear solver for minimizing the Huber norm: SEP–**103**, 281–289.

Kjems, U., Hansen, L. K., and Chen, C. T., 1996, A non-linear 3D brain co-registration method Proceedings of the Interdisciplinary Inversion Workshop 4. Methodology and Applications in Geophysics, Astronomy, Geodesy and Physics, Technical University of Denmark.

Nichols, D., 1994, Velocity-stack inversion using $\mathbf{L_p}$ norms: SEP–**82**, 1–16.

Rickett, J., and Lumley, D., 1998, A cross-equalization processing flow for off-the-shelf 4-D seismic data: 68th Ann. Internat. Meeting, Soc. Expl. Geophys., 16–19.

Rickett, J., 1999, On non-stationary convolution and inverse convolution: SEP–**102**, 129–136.

Robinson, E. A., and Treitel, S., 1980, Geophysical signal analysis: Prentice-Hall.

Rothman, D. H., Levin, S. A., and Rocca, F., 1985, Residual migration - applications and limitations: Geophysics, **50**, 110–126.

Sava, P., 2000, Variable-velocity prestack Stolt residual migration with application to a North Sea dataset: SEP–**103**, 147–157.

Thorson, J. R., 1984, Velocity stack and slant stack inversion methods: SEP–**39**.

Toga, A. W., and Thompson, P. M., 1998, Brain warping:, *in* Brain Warping Academic Press, 1–26.

Vaillant, L., 1999, Elf L7d North Sea 3-D dataset: SEP Data Library.

Wolberg, G., 1990, Digital image warping: IEEE Computer Society.